2017

The *Magnaporthe oryzae* nitrooxidative stress response suppresses rice innate immunity during blast disease

Margarita Marroquin-Guzman
University of Nebraska-Lincoln, mmarroquinguzman2@unl.edu

David E. Hartline
University of Nebraska-Lincoln, david.hartline@unl.edu

Janet D. Wright
University of Nebraska-Lincoln, jwright5@unl.edu

Christian G. Elowsky
University of Nebraska-Lincoln, celowsky@unl.edu

Travis J. Bourret
Creighton University

See next page for additional authors

Published in *Nature Microbiology* 2 (2017), 17054. doi 10.1038/nmicrobiol.2017.54

Submitted 20 December 2016; accepted 10 March 2017; published 18 April 2017

PMID: 28418377

The *Magnaporthe oryzae* nitrooxidative stress response suppresses rice innate immunity during blast disease

Margarita Marroquin-Guzman,[1] David Hartline,[1] Janet D. Wright,[1] Christian Elowsky,[2] Travis J. Bourret,[3] and Richard A. Wilson[1]

1 Department of Plant Pathology, University of Nebraska-Lincoln, Lincoln, Nebraska 68583
2 Department of Agronomy and Horticulture, University of Nebraska–Lincoln, Lincoln, Nebraska 68583
3 Department of Medical Microbiology and Immunology, Creighton University, Omaha, Nebraska 68178

Corresponding author — R. A. Wilson, rwilson10@unl.edu

Abstract

Understanding how microorganisms manipulate plant innate immunity and colonize host cells is a major goal of plant pathology. Here, we report that the fungal nitrooxidative stress response suppresses host defenses to facilitate the growth and development of the important rice pathogen *Magnaporthe oryzae* in leaf cells. Nitronate monooxygenases encoded by *NMO* genes catalyze the oxidative denitrification of nitroalkanes. We show that the *M. oryzae NMO2* gene is required for mitigating damaging lipid nitration under nitrooxidative stress conditions and, consequently, for using nitrate and nitrite as nitrogen sources. On plants, the Δ*nmo2* mutant strain penetrated host cuticles like wild type, but invasive hyphal growth in rice cells was restricted and elicited plant immune responses that included the formation of cellular deposits and a host reactive oxygen species burst. Development of the *M. oryzae* effector-secreting biotrophic interfacial complex (BIC) was misregulated in the Δ*nmo2* mutant. Inhibiting or quenching host reactive oxygen species suppressed rice innate immune responses and allowed the Δ*nmo2* mutant to grow and develop normally in infected cells. *NMO2* is thus essential for mitigating nitrooxidative cellular damage and, in rice cells, maintaining redox balance to avoid triggering plant defenses that impact *M. oryzae* growth and BIC development.

Global rice yields are significantly and negatively impacted each year by blast disease caused by the hemibiotrophic fungus *Magnaporthe oryzae*[1–3] (synonym of *Pyricularia oryzae*). Defining the full spectrum of molecular pro-

cesses used by *M. oryzae* to manipulate rice innate immunity and allow fungal colonization of host cells might reveal additional sources of pathogen resistance and improve crop health. *M. oryzae* infects hosts by first forming specialized infection structures, appressoria, at the tips of germ tubes emerging from spores adhered to the leaf surface.[4,5] A thin penetration peg emerging from an unmelanized patch on the base of the appressorium[6] is forced through the rice leaf cuticle under hydrostatic turgor pressure[1]. In the first penetrated cell, the peg differentiates into primary hyphae then bulbous invasive hyphae (IH) that are surrounded by the plant-derived extra-invasive hyphal membrane (EIHM). Branching IH fill the first invaded cell before spreading into neighboring living rice cells at around 44 h post-inoculation.[7,8] This biotrophic growth phase progresses for 4–5 days before *M. oryzae* enters its necrotrophic phase.

To colonize rice cells, *M. oryzae* must first suppress or avoid triggering two types of plant innate immunity that protect against microbial attack[9–11]: pathogen-associated molecular pattern (PAMP) triggered immunity (PTI), which can be suppressed by microbial effectors, and effector-triggered immunity (ETI), if effectors are detected. The biotrophic interfacial complex (BIC), a host membrane-derived structure, is formed behind *M. oryzae* IH in each invaded cell and is involved in deploying cytoplasmic effectors (with probable roles in suppressing host immunity) into rice cells.[11] Apoplastic effectors (that prevent fungal chitin recognition,[10] for example) are delivered by the conventional endoplasmic reticulum (ER)–Golgi secretion pathway to the apoplastic space and accumulate between the fungal cell wall and the EIHM (ref. 10).

How fungal growth and development are integrated with sustained plant defense suppression during the first four to five days of biotrophy is largely unresolved at the molecular level.[2,12] The host reactive oxygen species (ROS) burst is common to PTI and ETI and must be neutralized by fungal antioxidation components during compatible interactions between *M. oryzae* and rice or barley to prevent the induction of basal plant defenses.[13–16] The *M. oryzae* glucose-6-phosphate (G6P) sensor, Tps1, regulates carbon metabolism and connects glucose availability[17] to glutathione-dependent antioxidation and the establishment of biotrophy.[18] Other examples linking fungal metabolic regulation and plant defense suppression are not known. We hypothesized that nitrogen-regulated processes might also contribute to the colonization of rice cells by *M. oryzae*. Here, we report that a fungal nitronate monooxygenase is nitrogen and carbon-regulated, mitigates nitrooxidative stress and, in plants, maintains host redox balance. This latter action prevents the triggering of rice innate immunity and facilitates *M. oryzae* growth and BIC development in rice cells.

Results

NMO2, encoding a nitronate monooxygenase, is expressed in a Tps1- and Nut1-dependent manner and is required for nitrate utilization. We were intrigued that the *M. oryzae* genome[19] carries five *NMO* genes encoding putative nitronate monooxygenase enzymes that catalyze the oxidative denitrification of nitroalkanes to their corresponding carbonyl compounds and nitrite (NO_2^-, Fig. 1a): MGG_07261 (*NMO1*); MGG_02439 (*NMO2*), MGG_02593 (*NMO3*), MGG_09511 (*NMO4*) and MGG_01473 (*NMO5*). To our knowledge, *NMO* genes have not been functionally characterized in fungi. To determine which, if any, might be involved in pathogenicity, we hypothesized that physiologically relevant *NMO* genes might be expressed under the control of the nitrogen regulator Nut1. Our reasoning was twofold. First, Nut1, like other GATA-family nitrogen regulators,[20] is required in *M. oryzae* for derepressing the expression of genes involved in the utilization of nitrogen sources other than ammonium (NH_4^+). Nitroalkanes could conceivably be used as alternative nitrogen sources, because oxidative denitrification yields NO_2^- (Fig. 1a). Second, NO_2^- would be assimilated into amino acids following its reduction to NH_4^+ by nitrite reductase encoded by *NII1*. *NII1* is expressed in a Nut1-dependent manner under nitrogen derepressing conditions.[17] It thus seemed logical that Nut1 would coordinate the oxidative denitrification of nitroalkanes with the reduction of NO_2^- to NH_4^+. We used quantitative real-time PCR (qPCR) to examine the expression of *NMO1–5* following axenic growth under nitrogen derepressing conditions in wild type (WT) and the Δ*nut1* mutant strain. Figure 1b shows that, after normalizing against the β-tubulin-encoding gene *TUB2*, *NMO2* and *NMO4* were expressed more than threefold higher in WT compared to the Δ*nut1* mutant strain on derepressing nitrogen media. Normalized fold expression changes for *NMO1*, *3* and *5* in WT compared to the Δ*nut1* mutant were less than two. Thus, *NMO2* and *NMO4* expression requires Nut1 for strong induction following axenic growth under nitrogen-derepressing conditions. Additionally, qPCR analysis of complementary DNA (cDNA) extracted from whole rice leaves inoculated with WT or the Δ*nut1* mutant showed that *NMO2* was expressed during early *in planta* colonization in a Nut1-dependent manner (Fig. 1c).

We focused on characterizing *NMO2* and *NMO4* and made deletion strains by homologous replacement of the respective genes with *ILV1* conferring sulfonyl urea resistance.[21] We could find no phenotype for the resulting Δ*nmo4* mutant strain, which was fully pathogenic on rice and, unlike Δ*nmo2*, showed no growth defects on nitrate media (Supplementary Fig. 1a,b). Consequently, we did not continue work on the Δ*nmo4* mutant strain. In contrast, growth testing on our defined 1% glucose (wt/vol) minimal medium (GMM) with NO_3^- as the sole nitrogen source revealed that

the Δ*nmo2* mutant was NO_3^- non-utilizing (Fig. 1d). Introducing a functional copy of *NMO2* into the Δ*nmo2* mutant strain restored NO_3^- utilization in the resulting Δ*nmo2 NMO2* complementation strain (Fig. 1d). The lack of growth of the Δ*nmo2* mutant on NO_3^- media was not due to changes in the expression of *NIA1* or *NII1* compared to WT (Fig. 1e). This suggested that *NMO2* was not epistatic to *NIA1* and *NII1*. Rather, during nitrate use, Nut1 induced *NMO2*, *NIA1* and *NII1* gene expression concomitantly. Furthermore, like *NIA1* (ref. 22), *NMO2* gene expression required the G6P sensor Tps1 (Fig. 1f). Taken together, Fig. 1g shows the deduced genetic relationships between G6P, the control of *NMO2* gene expression by Tps1 and Nut1, and nitrate metabolism.

***NMO2* is required for protection against nitrooxidative stress.**
We sought to understand why the Δ*nmo2* mutant strain was nitrate non-utilizing. To address this, we first compared the growth of WT and the Δ*nmo2* mutant on undefined complete medium (CM), and on defined GMM containing organic and inorganic sole nitrogen sources that support WT growth[5]. Figure 2 shows that, in addition to NO_3^- media, the Δ*nmo2* mutant was similarly impaired for growth on NO_2^- media. The sparse colonies produced by Δ*nmo2* on NO_3^- and NO_2^- media were not observed on any of the other growth media tested, although gamma aminobutyric acid (GABA) as a sole nitrogen source slightly impaired Δ*nmo2* radial growth compared to WT. Also, the sparse hyphal phenotype of Δ*nmo2* on NO_3^- and NO_2^- media was distinct from that observed for the Δ*nut1* mutant,[17] which is completely attenuated for growth on these media, probably because, in contrast to Δ*nmo2*, Δ*nut1* strains do not express *NIA1* and *NII1*.

To account for the poor growth of the Δ*nmo2* mutant on NO_3^- and NO_2^- media, we considered that the metabolism of these nitrogen sources generates reactive nitrogen species (RNS). Nitric oxide (NO) is produced as a by-product of nitrate metabolism.[23] NO reacts with ROS such as the superoxide anion to generate RNS, including peroxynitrite[24] (Fig. 3a). Peroxynitrite contributes to cellular nitrooxidative stress by reacting directly or indirectly with lipids and proteins in the cell.[24–27] In addition, NO_2^-, a higher oxide of NO and a source of RNS, induces lipid oxidation or nitration.[27,28] Because one outcome of RNS production is the generation of nitroalkanes and other nitrated lipid species[29] (Fig. 3a), we postulated that a functional Nmo2 protein might be required to mitigate RNS-induced lipid damage during growth on NO_3^- and NO_2^- media. Lipid nitration is difficult to measure and detect directly, due to the highly reactive nature of nitrated lipids.[25] Nonetheless, five lines of evidence support our hypothesis that the Nmo2 protein is required for neutralizing nitrooxidative cell stress. First, using 2-nitropropane as a substrate, Nmo enzyme activity was detected in WT but not in Δ*nmo2* whole-cell protein extracts (Fig. 3b). This confirms *NMO2* encodes a bone

fide nitronate monooxygenase. Second, the Δ*nmo2* mutant strain was sensitive to both NO (from the NO donor sodium nitroprusside, Fig. 3c) and ROS (as H_2O_2, Fig. 3d), two determinants of RNS production (Fig. 3a). Third, the growth of the Δ*nmo2* mutant on NO_3^- medium was markedly improved, relative to WT, in the presence of the peroxynitrite scavenger MnTBAP chloride[30] (Fig. 3e and Supplementary Fig. 2a). Fourth, the concentration of malondialdehyde (MDA), a marker for lipid damage (that is, peroxidation and/or nitration) induced by RNS such as peroxynitrite or $NO_2^{\bullet}$ (ref. 31), was significantly increased in the mycelia of Δ*nmo2* compared to WT following growth on NO_3^- medium (Fig. 3f). This suggests that higher oxides of NO such as peroxynitrite are more damaging to cell membranes in the Δ*nmo2* mutant than in WT. Fifth, nitrotyrosine levels were elevated in the Δ*nmo2* mutant compared to WT following growth on NO_3^- media (Fig. 3g). Nitrotyrosine is a biological marker for nitrooxidative stress[32] and accumulates in the presence of high levels of RNS. Taken together, loss of 2-nitroporopane metabolism, sensitivity to NO and ROS, improved growth on NO_3^- medium with a peroxynitrite scavenger, high levels of MDA indicating lipid damage and the accumulation of nitrotyrosine in the Δ*nmo2* mutant strain all support the notion that Nmo2 protects against nitrooxidative stress by denitrifying nitrated alkanes and lipids. This mitigating role of *NMO2* explains why the Δ*nmo2* mutant was unable to grow on RNS-generating NO_3^- or NO_2^- media but grew well with NH_4^+ and amino acids as sole nitrogen sources.

NMO2 is essential for rice blast disease.

The Δ*ndo2* mutant strain sporulated less than WT on CM (Supplementary Fig. 2b), but enough conidia could be harvested for downstream applications. We applied spores of the Δ*nmo2* mutant to three-week-old rice plants of the susceptible cultivar CO-39. Compared to WT and the Δ*nmo2 NMO2* complementation strain, the loss of *NMO2* function abolished foliar infection by *M. oryzae* (Fig. 4a). Using optically clear rice leaf sheaths, we determined that the loss of pathogenicity by the Δ*nmo2* mutant was not due to appressorial defects, because both the rate of appressorial formation on the rice leaf surface (Supplementary Fig. 3a) and the rate of penetration into rice cells (Supplementary Fig. 3b) were not significantly different between Δ*nmo2* and WT. However, Δ*nmo2* IH did not fill the first infected cell, and the movement of IH into rice cells adjacent to the first penetrated cell was significantly reduced compared to WT (Supplementary Fig. 3c). These results indicate that biotrophic growth was attenuated in the Δ*nmo2* mutant and, when taken together, we conclude that *NMO2* is not required for appressorium formation or function but is an *in planta*-specific determinant of biotrophic growth in rice cells. Strikingly, the poor biotrophic growth of Δ*nmo2* IH resulting from the loss of *NMO2* function was accompanied by the formation of granular depositions in rice cells. These cellular deposits were

not observed in rice cells infected with either WT (Fig. 4b) or the Δ*nut1* mutant strain downregulated for *NMO2* expression (Supplementary Fig. 3d), although *in planta* Δ*nut1* IH growth was also impaired. How the downregulation (as opposed to the loss) of *NMO2* function contributes to the reduced growth of Δ*nut1* in rice cells compared to other metabolic perturbations in this mutant strain is not known at this time.

NMO2 is required to suppress rice cell defenses.

To understand how the loss of *NMO2* attenuated *M. oryzae* biotrophic growth, we first hypothesized that the observed granules in rice cells infected with Δ*nmo2* IH (Fig. 4b) resulted from induced plant defense responses. Our rationale for this hypothesis was based on our previous observations that a sirtuin-family protein, MoSir2, regulates superoxide dismutase (SOD) gene expression via a histone hydroxylase-family member, MoJmjC (ref. 16). Subsequently, we showed that Δ*sir2* mutant strains were impaired in neutralizing the host ROS burst, such that during Δ*sir2* IH growth in rice cells, ROS accumulated and triggered plant defenses including the formation of granular depositions[16]. To test our hypothesis regarding Δ*nmo2*, we examined the accumulation of ROS in WT and Δ*nmo2* IH infected rice cells by staining for hydrogen peroxide (H2O2) accumulation with 3,3′-diaminobenzidine (DAB). Figure 4c shows that rice cells infected with Δ*nmo2* IH (but not WT IH) were strongly stained with DAB. This result confirmed that, in addition to granular deposits (Fig. 4b), rice cells colonized with Δ*nmo2* IH also accumulated ROS (Fig. 4c).

ROS accumulation in rice cells has previously been shown to induce the expression of plant defense genes.[13,16] Figure 4d shows that cells infected with Δ*nmo2* IH were upregulated for the expression of the pathogenesis-related (PR) genes *PBZ1* and *PR-1* compared to WT infected cells. Moreover, callose was observed accumulating in the walls of rice cells infected with Δ*nmo2* but not WT strains (Supplementary Fig. 3f), and the rice callose synthase-encoding genes *OsGSL1*, *OsGSL3* and *OsGSL5* (ref. 33) were upregulated in rice leaf sheaths challenged with Δ*nmo2* compared to WT (Supplementary Fig. 3g). We conclude that, compared to WT, rice cells infected with Δ*nmo2* IH accumulated ROS, formed callose depositions and expressed defense genes. *NMO2* is thus required for suppressing the rice innate immune response during *M. oryzae* infection.

NMO2 is required to maintain redox balance in *M. oryzae* infected rice cells to avoid triggering host innate immunity.

To determine if ROS accumulation in rice cells infected with the Δ*nmo2* mutant was the trigger for the observed rice innate immune responses, we treated spores of the Δ*nmo2* mutant (Fig. 4e,f) and WT (Supplementary Fig. 3g and Fig. 4f) with the NADPH oxidase inhibitor diphenyleneiodonium

(DPI), or with the ROS scavenger ascorbate (Supplementary Fig. 3h,i), at concentrations that had previously been determined not to affect appressorium formation or function,[16] and applied them to the surface of rice leaf sheaths. Compared to untreated controls, treatment with DPI (Fig. 4e) or ascorbate (Supplementary Fig. 3h) prevented granule formation in Δ*nmo2* infected rice cells. These results indicate that *NMO2* was required to maintain redox balance and prevent or neutralize the host ROS burst to avoid triggering downstream plant defenses. Moreover, with both treatments, the movement of Δ*nmo2* IH to cells adjacent to the point of infection was significantly increased at 42 h.p.i. (hours post inoculation) compared to untreated controls (Fig. 4f and Supplementary Fig. 3i). This demonstrated that the attenuated biotrophic growth of Δ*nmo2* mutant strains was due to induced rice innate immune responses resulting from host ROS accumulation rather than stemming from a requirement for *NMO2* in fungal biotrophic growth *per se*.

Induced host innate immunity perturbs Δ*nmo2* BIC formation in rice cells.

We next asked whether the induced plant defenses in response to Δ*nmo2* infection were sufficient to kill the fungus or otherwise affect development. Such information could be used to probe how plant cells contain or destroy invaders. We transformed WT and the Δ*nmo2* mutant strain with pBV591 (ref. 11) to produce strains expressing the apoplastic effector Bas4 fused to green fluorescent protein (Bas4:GFP) and the BIC-accumulating cytoplasmic effector Pwl2 fused to mCherry and a rice nuclear localization signal (Pwl2:mCherry:NLS). We screened for transformants expressing both effectors by live-cell imaging of infected leaf sheaths using scanning confocal microscopy. Figure 5 shows that, during early infection at 32 h.p.i., WT accumulated Bas4:GFP in the apoplast where it outlines IH, and localized Pwl2:mCherry:NLS to a single, punctate BIC, as described previously.[11,34] In contrast, Δ*nmo2* mutant strains expressing Bas4:GFP and Pwl2:mCherry:NLS began to elicit granular depositions in rice cells by 32 h.p.i. (Fig. 5) and, although Bas4: GFP outlined IH in Δ*nmo2* mutant strains (indicating that secretion of this effector into the apoplast was not impaired by the plant response), Pwl2:mCherry:NLS localized to several foci and was also dispersed throughout IH, indicating that BIC development and cytoplasmic effector secretion were perturbed in this strain. By 38 h.p.i., the developmental differences between WT and Δ*nmo2* strains in rice cells were more pronounced. Figure 6 (top panel) shows that Δ*nmo2* mutant strains expressing Bas4:GFP and Pwl2:mCherry:NLS elicited strong plant defense responses and granular depositions in rice cells. Like WT, the Δ*nmo2* mutant strains continued to secrete Bas4:GFP into the apoplast. However, unlike for WT, Pwl2:mCherry:NLS localized to multiple foci in the sparse Δ*nmo2* IH. Despite this striking perturbation in BIC formation, Pwl2:mCherry:NLS was nonetheless secreted from Δ*nmo2* IH into the host cytoplasm and accumulated in rice nuclei (Fig. 6).

We hypothesized that multi-BIC formation in Δ*nmo2* mutant strains was a developmental stress response resulting from exposure to the host ROS burst and/or other induced plant defenses. In support of this notion, Fig. 6 (bottom panel) shows how inhibiting the host ROS burst with DPI treatment remediated BIC formation in Δ*nmo2* mutant strains and restored the accumulation of Pwl2:mCherry:NLS to focal BICs. Bas4:GFP secretion in Δ*nmo2* mutant strains and Pwl2:mCherry:NLS and Bas4:GFP secretion in WT strains were not affected by DPI treatment. We conclude that, in the face of the host ROS burst and the induction of plant defenses resulting from loss of the fungal nitrooxidative stress response, Δ*nmo2* continues to secrete effectors, but BIC development and IH growth are perturbed. Solely preventing the host ROS burst ameliorates these physiological defects. These results dissect the fine-tuned molecular and cellular interplay between host and pathogen that governs disease progression in rice, and provide a vantage point for understanding the determinants of fungal development in the context of the host cell environment.

Discussion

This work provides insights into two key fungal processes: (1) how the fungal cell is protected from nitrooxidative stress by a nitronate monooxygenase, Nmo2, during growth under RNS-inducing conditions, and (2) how the fungus requires Nmo2 to suppress the first line of plant defenses against microbial pathogens. Nmo2 acts to catalyze the oxidative denitrification of nitroalkanes. The loss of *NMO2* resulted in increased lipid and protein nitration, poor growth on NO_3^- and NO_2^- media and increased sensitivity to NO and H2O2. Growth on NO_3^- medium was markedly improved by the addition of a peroxynitrite scavenger. The requirement for *NMO2* in neutralizing RNS-induced cellular damage during growth on NO_3^- and NO_2^- media explains *NMO2* expression control by nitrogen metabolite repression. Deducing that *NMO2* is expressed under nitrogen derepressing and glucose-inducing conditions (via Nut1 and Tps1, respectively) is important, because, although fungal responses to ROS are well established, little is known about the regulation of fungal RNS responses.[35] During host infection, the loss of *NMO2* caused a host ROS burst that triggered rice innate immunity, resulting in multi-BIC development and impaired biotrophic growth. Remediation of Δ*nmo2* physiological defects by DPI treatment showed that the major role of *NMO2* during early infection was to maintain redox balance in rice cells. Whether this is achieved by preventing or, alternatively, neutralizing the host ROS burst is currently unknown. Nmo2 might be required to mitigate lipid damage resulting either directly or indirectly from RNS, as a means of quenching ROS. Alternatively, during the denitrification reaction, superoxide can be the source of incorporated O_2 (ref. 36 and Fig. 1a). ROS could thus

be consumed directly by Nmo2 (as superoxide) during this reaction. Perturbations to either of these processes in Δ*nmo2* mutant strains could result in ROS accumulation in rice cells and the triggering of innate immunity. Repairing lipid nitrooxidative damage might also prevent the amplification of host ROS by some currently unknown mechanism. Furthermore, compared to ROS, much less is known about plant NO metabolism. NO is a component of the plant immune response and can react with ROS to produce plant RNS (ref. 37). However, our results—obtained from inhibiting ROS by DPI—suggest that plant RNS compounds or plant NO signaling are not effective inhibitors of *M. oryzae* in the absence of a host ROS burst. Conversely, in the presence of a host ROS burst, effectors secreted by Δ*nmo2* mutant strains do not suppress PTI. These results, taken together, question the primacy of secreted effectors in suppressing host signaling and defense responses and form starting points for further dissecting the hierarchy of molecular events leading to plant innate immunity. When taken together, we describe essential roles for *NMO2* in suppressing host innate immunity and establishing biotrophic growth in rice cells. We thus provide insight into a previously unknown aspect of molecular host–microorganism interactions and, more broadly, identify a new requisite for nitrate and nitrite metabolism in fungi.

Methods

Strains and culture conditions. The *M. oryzae* wild-type strain Guy11 was used throughout as both a control strain and as a parental strain for the mutants generated during the course of this study (Supplementary Table 1). All strains are available from the Wilson laboratory as filter stocks. During the course of the study, strains were propagated on complete media.[38] Strains were growth-tested on defined minimal medium containing 1% (wt/vol) glucose (GMM), with indicated nitrogen sources, as previously described.[21] Strains were tested for susceptibility to nitrooxidative stress on CM with H_2O_2 (30% in water, Fisher) and sodium nitroprusside dehydrate (NPS, MP Biomedicals) at the indicated concentrations. The peroxynitrite scavenger MnTBAP chloride (AdipoGen Life Sciences) was added to GMM with 10 mM NO_3^- as the sole nitrogen source. All strains were grown at 24 °C with 12 h light/dark cycles. Plate images were taken at the indicated time points with a Sony Cyber-shot digital camera 14.1 megapixels.

Gene transcript analysis. Gene transcript analysis was performed on cDNAs obtained from fungal mycelia and infected rice leaf sheaths or whole leaves, as previously described by Fernandez and associates.[16] For *in planta* gene transcript analysis, infected plant tissue was frozen in liquid nitrogen at the indicated time points and ground with a mortar and pestle. Mycelial samples were collected from the indicated liquid growth media and lyophilized for 36 h before grinding. RNA was extracted from ~100 mg of leaf or mycelial tissue using the RNeasy mini kit (Qiagen). DNase I (Invitrogen) treatment was applied to 1 µg of RNA per sample, and cDNA was generated using qScript (Quantas). qPCR was performed on an Eppendorf Mas-

tercycler Realplex using the primers described in Supplementary Table 2 and the following conditions: 10 min at 95 °C, followed by 40 cycles of 95 °C for 30 s, 63 °C for 30 s and 72 °C for 30 s.

Gene functional analysis. Targeted gene replacement of the *M. oryzae NMO* genes was achieved using the split marker strategy described by Wilson and associates.[21] Briefly, the sequence of the *NMO2,4* genes was obtained from the *M. oryzae* genome database at the Broad Institute and was used to design gene-specific primers (Supplementary Table 2). A total of 1 kb of the gene of interest was replaced with the sulfonylurea resistance-conferring gene, *ILV1* (2.8 kb). Targeted gene deletion was confirmed for two transformants by PCR (ref. 21), which were subsequently tested for pathogenicity on rice seedlings. To ensure that the Δ*nmo2* phenotype resulted solely from targeted replacement of the *NMO2* gene, the full-length *NMO2* gene (plus 1 kb each of 5′ and 3′ flanking sequences) was amplified by PCR using the primers listed in Supplementary Table 2 and transformed into protoplasts of one of the Δ*nmo2* mutant strains. Five Δ*nmo2 NMO2* complementation strains were selected by their growth on GMM with nitrate as a nitrogen source. Two were tested for restored pathogenicity on host plants. Strains expressing Bas4:GFP and Pwl2:mCherry:NLS were generated by transforming WT and Δ*nmo2* mutant strains with pBV591 (ref. 11) and selecting for hygromycin resistance. Positive strains were initially identified by PCR using primers designed to amplify the *Hph* gene (Supplementary Table 2). Ten transformants from each parental strain were subsequently screened for the expression of both apoplastic Bas4:GFP and cytoplasmic Pwl2:mCherry:NLS during rice leaf sheath infection using laser scanning confocal microscopy.

Nitronate monooxygenase enzyme activity assay. WT and Δ*nmo2* strains were grown in CM medium for 48 h and switched to NO_3^- medium for 16 h. Proteins were extracted from lyophilized mycelia as described previously.[22] Nmo enzyme activity was assayed as previously described.[39] Briefly, 50 μM 2-nitropropane was added to each protein sample and the rate of NO_2^- product formed was measured using the absorbance of light with a wavelength of 540 nm following color development resulting from the reaction of NO_2^- with sulfanilamide (Sigma) and *N*-1-(naphthyl) ethylenediamine dihydrochloride (Sigma).

Detection of nitrooxidative damage. WT and Δ*nmo*2 strains were grown in 350 ml CM. After 48 h, the mycelia were collected and transferred to flasks containing 100 ml of 1% (wt/vol)GMM with 10 mM NO_3^- as the sole nitrogen source. Mycelial samples were shaken for 16 h, collected again, and lyophilized for 36 h.

Nitrotyrosine formation was determined for WT and the Δ*nmo2* strains grown with NO_3^- as the sole nitrogen source. Briefly, 10 mg of mycelia were resuspended in 1 ml alkaline lysis buffer (25 mM Tris, 100 mM SDS and 128 mM NaOH) in a tube containing 3.0 mm zirconium beads and were homogenized using a Beadbug Microtube Homogenizer (Benchmark Scientific). The protein concentrations from the mycelial cell lysates were determined using the Pierce BCA Protein Assay Kit (Thermo Scientific) and normalized to a concentration of 1.25 mg ml^{-1} in Laemmli sample buffer with 2-mercaptoethanol. Proteins were separated on an AnyKD TGX polyacrylamide gel and transferred to a PVDF membrane using a Transblot Turbo Trans-

fer System (Bio-Rad Laboratories). The PVDF membrane was blocked with 5% non-fat dry milk in tris-buffered saline with 0.1% Tween-20 (TBST) (0.1% Tween-20, 150 mM NaCl, 100 mM Tris, pH 7.5) buffer. Proteins were probed with a 1:1,000 dilution of an anti-nitrotyrosine polyclonal antibody (Thermo Scientific) and then washed five times with TBST. PVDF membranes were incubated with a 1:2,000 dilution of a horseradish peroxidase (HRP)-conjugated goat anti-rabbit IgG secondary antibody and then washed five times with TBST. Immunoreactive proteins were visualized using the WesternSure Enhanced Chemiluminescence (ECL) Kit on a C-DiGit Blot Scanner (LI-COR).

Damage to cell membranes was assessed by measuring the concentration of malondialdehyde (MDA) using the TBARS Assay Kit (Cayman). Mycelia (25 mg) were homogenized in HN (20 mM NaCl, 50 mM HEPES, pH 7.6) buffer using zirconium beads as described above. Samples were centrifuged for 1 min to pellet cell debris and 100 µl of cell lysates were mixed with 100 µl SDS. Samples were then added to 4 ml of MDA colorometric reagent, boiled for 1 h and then quenched on ice for 10 min. Samples were read at 450 nm on a Cytation 5 multimode reader (BioTek) and the concentration of MDA was determined using standards included in the TBARS Assay Kit.

Pathogenicity tests and live-cell imaging. Plant infection assays were performed on three- to four-week-old rice seedlings (*Oryza sativa*) of the susceptible cultivar CO-39 by spraying 10 ml of conidial suspensions (1×10^5 spores ml^{-1}) in 0.2% gelatin (Difco). Infected plants were placed in darkness overnight at 26 °C and then transferred to a growth chamber with 12 h light/dark periods at 26 °C for five to seven days. Images of infected leaves were taken at a resolution of 600 d.p.i., using an Epson Perfection V550 Photo scanner.

Live-cell imaging was performed in a Nikon A1 laser scanning confocal mounted on a Nikon 90i compound microscope (software version: NIS-Elements 4.40.00). The images were taken with a ×60 objective with a ×2 digital zoom. Transmitted light was used for phase contrast images. The filter settings were as follows: GFP (excitation 488 nm, emission 500–550 nm), mCherry (excitation 561 nm emission 575–625 nm). For 3,3′-diaminobenzidine (DAB, Sigma-Aldrich) staining, infected rice sheaths were collected at 42 h.p.i. and incubated in 1 mg ml–1 DAB solution (pH 3.8) at room temperature for 8 h in the dark.[16] After incubation, samples were destained with ethanol:acetic acid (94:4, vol/vol) for 1 h. Images were taken with a Leica DC300 camera mounted on a Leica DMLB microscope at ×400 magnification. For callose staining, rice sheaths were cleared overnight with ethanol: acetic acid (6:1, vol/vol). Subsequently, the samples were rehydrated and stained with 0.05% (wt/vol) aniline blue (Acros Organics) in 0.067 M K2HPO4 buffer at pH 9.2 for 6 h. Images were taking using 405 nm excitation and 500–550 nm emission. L-Ascorbic acid sodium salt (Acros Organics) and the NADPH oxidase inhibitor diphenylene iodonium (DPI, Sigma-Aldrich) were added to spore suspensions at the stated concentrations before inoculating rice sheaths. Statistical comparisons among the strains were performed with Graph Pad Prism (v.6).

Data availability — The data that support the findings of this study are available from the corresponding author upon request.

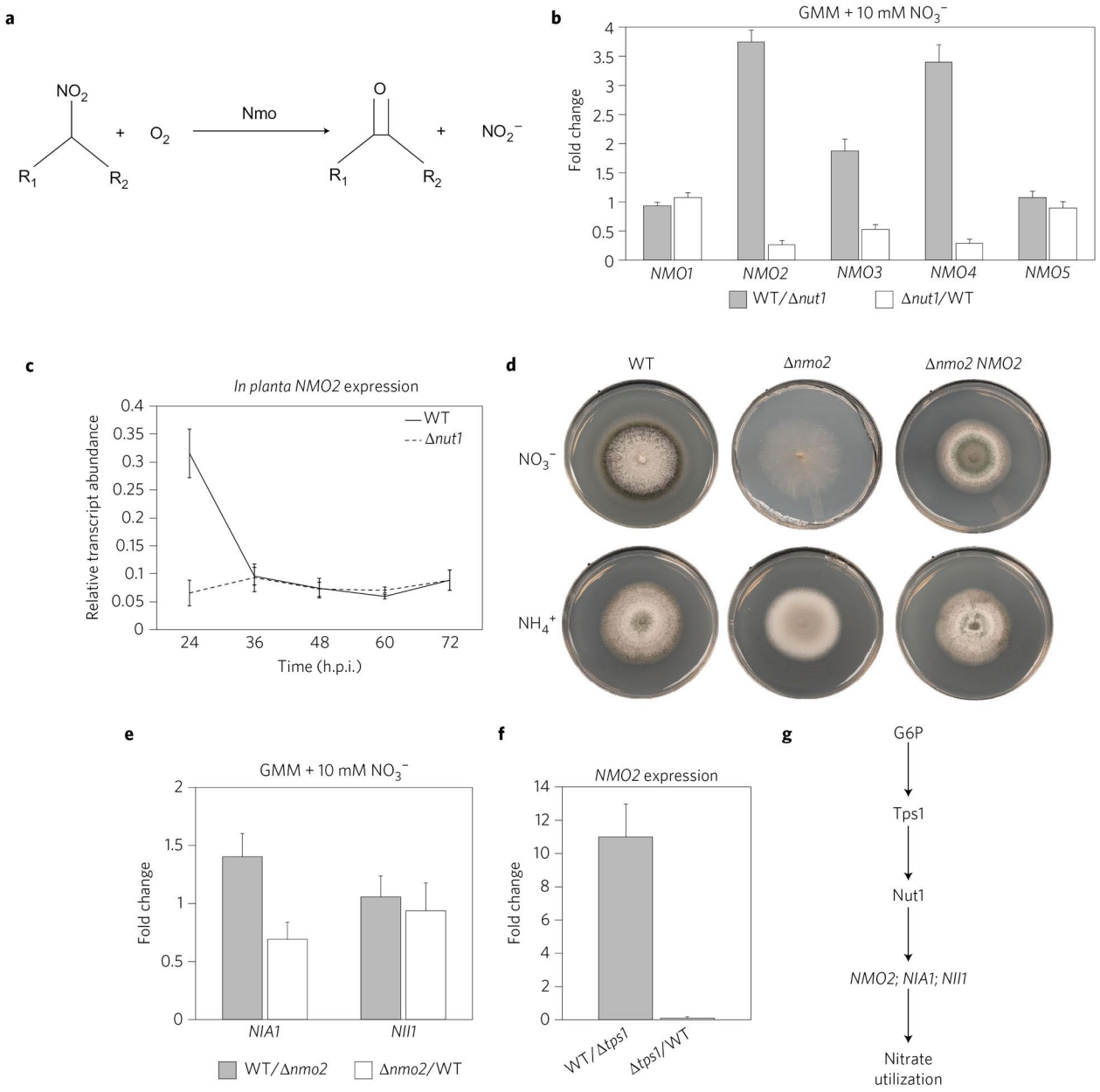

Figure 1. *NMO2*, encoding a nitronate monooxygenase, is required for nitrate utilization. **a)** Nitronate monooxygenase (Nmo) uses molecular oxygen to oxidize alkyl nitronates to the corresponding carbonyl compounds and nitrite. R_1 = H or alkyl group, R_2=H or CH_3. **b)** The expression of *NMO* genes was analyzed in wild type (WT) and the Δ*nut1* mutant after 16 h of growth in defined minimal medium containing 1% (wt/vol) glucose (GMM) and 10 mM NO_3^- as the sole nitrogen source (NO_3^- medium). **c)** Expression of *NMO2* was Nut1-dependent during early biotrophy. RNA was extracted from spray-inoculated leaves of whole rice seedlings at the indicated time points. *NMO2* expression was normalized against the *MoACT1* gene and the values are the average of two biological replicates consisting of three technical replicates each. Error bars indicate standard deviation. **d)** Plate tests of WT, Δ*nmo2* mutant and Δ*nmo2 NMO2* complementation strains after ten days of growth on 85 mm Petri dishes with GMM and 10 mM of the indicated sole nitrogen source. Each plate test was performed in triplicate with one representative plate selected for imaging. **e)** The expression of *NIA1* and *NII1* was similar in WT and Δ*nmo2* strains following 16 h of growth in GMM with 10 mM NO_3^-. **f)** *NMO2* was expressed in a Tps1-dependent manner following growth on GMM with 10 mM NO_3^-. In **b**,**e**,**f**, gene expression averages were normalized against the *M. oryzae TUB2* gene and fold changes were calculated between strains. Values are the average of two biological replicates each with three technical replicates. Error bars indicate standard deviation. **g)** Model of *NMO2* gene expression control and role in nitrate use.

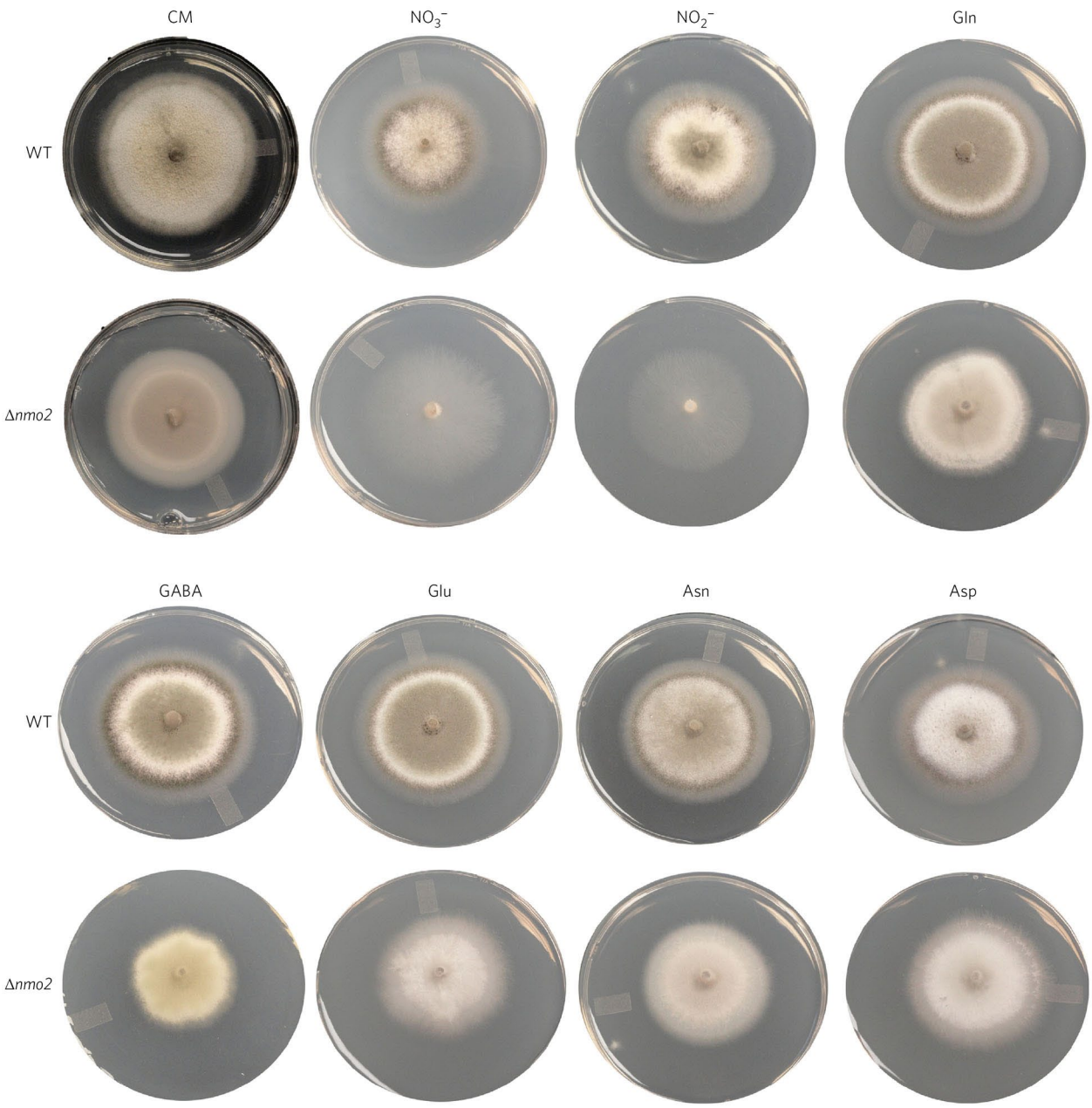

Figure 2. *NMO2* is required for growth on media containing nitrate or nitrite as the sole nitrogen source. WT and Δ*nmo2* mutant strains were grown on complete medium (CM) and on defined 1% (wt/vol) GMM with 10 mM of the indicated sole nitrogen source. L isomers were used throughout this study. Growth tests were performed in triplicate using 85 mm Petri dishes. One representative plate of each treatment and strain was imaged after ten days of growth.

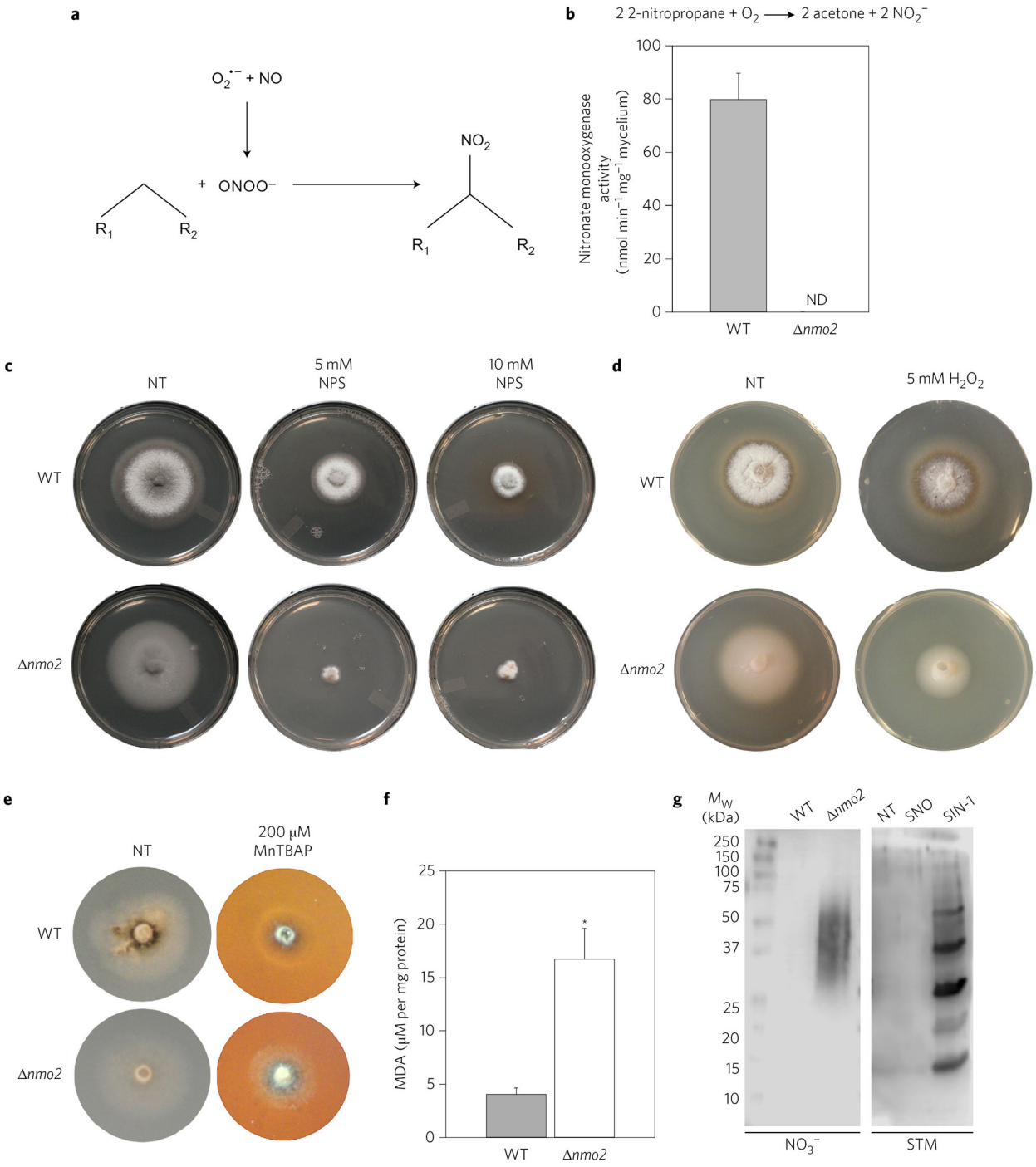
a
$O_2^{\bullet-}$ + NO
+ ONOO⁻
NO_2
R_1
R_2
R_1
R_2
b
2 2-nitropropane + O_2 ⟶ 2 acetone + 2 NO_2^-
Nitronate monooxygenase activity (nmol min^{-1} mg^{-1} mycelium)
100
80
60
40
20
0
ND
WT
Δnmo2
c
NT
5 mM NPS
10 mM NPS
WT
Δnmo2
d
NT
5 mM H_2O_2
WT
Δnmo2
e
NT
200 μM MnTBAP
WT
Δnmo2
f
MDA (μM per mg protein)
25
20
15
10
5
0
*
WT
Δnmo2
g
M_W (kDa)
WT
Δnmo2
NT
SNO
SIN-1
250
150
100
75
50
37
25
20
15
10
NO_3^-
STM

Figure 3. *NMO2* is required for tolerating nitrooxidative stress. **a)** Nitric oxide (NO) and other reactive nitrogen species (RNS) can react with superoxide ($O_2^{\bullet -}$) to produce peroxynitrite ($ONOO^-$), which can result in lipid nitration.[25] **b)** Nitronate monooxygenase activity was measured in WT and Δ*nmo2* strains following 48 h growth in CM and 16 h growth in GMM with NO_3^-. Enzyme activity was determined spectrophotometrically ($A_{540\ nm}$), in triplicate, using 2-nitropropane as substrate. Activity was calculated from the concentration of NO_2^- produced in 1 min by whole-cell protein extracts from 100 mg of mycelium. ND, not detected. Error bars indicate standard deviation. **c)** The Δ*nmo2* mutant was sensitive to the NO donor sodium nitroprusside dihydrate[40] (NPS) compared to WT. Plates were imaged after eight days of growth in the dark. **d)** The Δ*nmo2* mutant was sensitive to exogenous ROS compared to WT. CM plates with or without 5 mM H_2O_2 were inoculated with the indicated strains and imaged after five days of growth. In **c** and **d**, 55 mm Petri dishes were used. **e)** The Δ*nmo2* mutant was restored for growth on RNS-generating NO_3^- medium, relative to WT, by adding the peroxynitrite scavenger MnTBAP. For clarity, images taken after five days of growth were cropped from 85 mm plates (Supplementary Fig. 2a). NT, no treatment control. Each plate test was performed in triplicate with one representative plate used for imaging. **f)** The levels of malondialdehyde (MDA) were determined for WT and the Δ*nmo2* mutant strain following growth in the presence of NO_3^- as a sole nitrogen source. *$P < 0.0001$ (two-tailed *t*-test) compared with WT. Values are the average of four technical replicates and two biological replicates, with standard deviation. **g)** An immunoblot for nitrotyrosine was performed on cell lysates produced from WT and Δ*nmo2* strains. As a standard positive control, the formation of nitrotyrosine was determined for cell lysates produced from *Salmonella enterica* serovar Typhimurium strain 14028s (STM) that were either not treated (NT) or exposed to 2.5 mM of the NO donor spermine NONOate (SNO) or the $ONOO^-$ generator SIN-1.

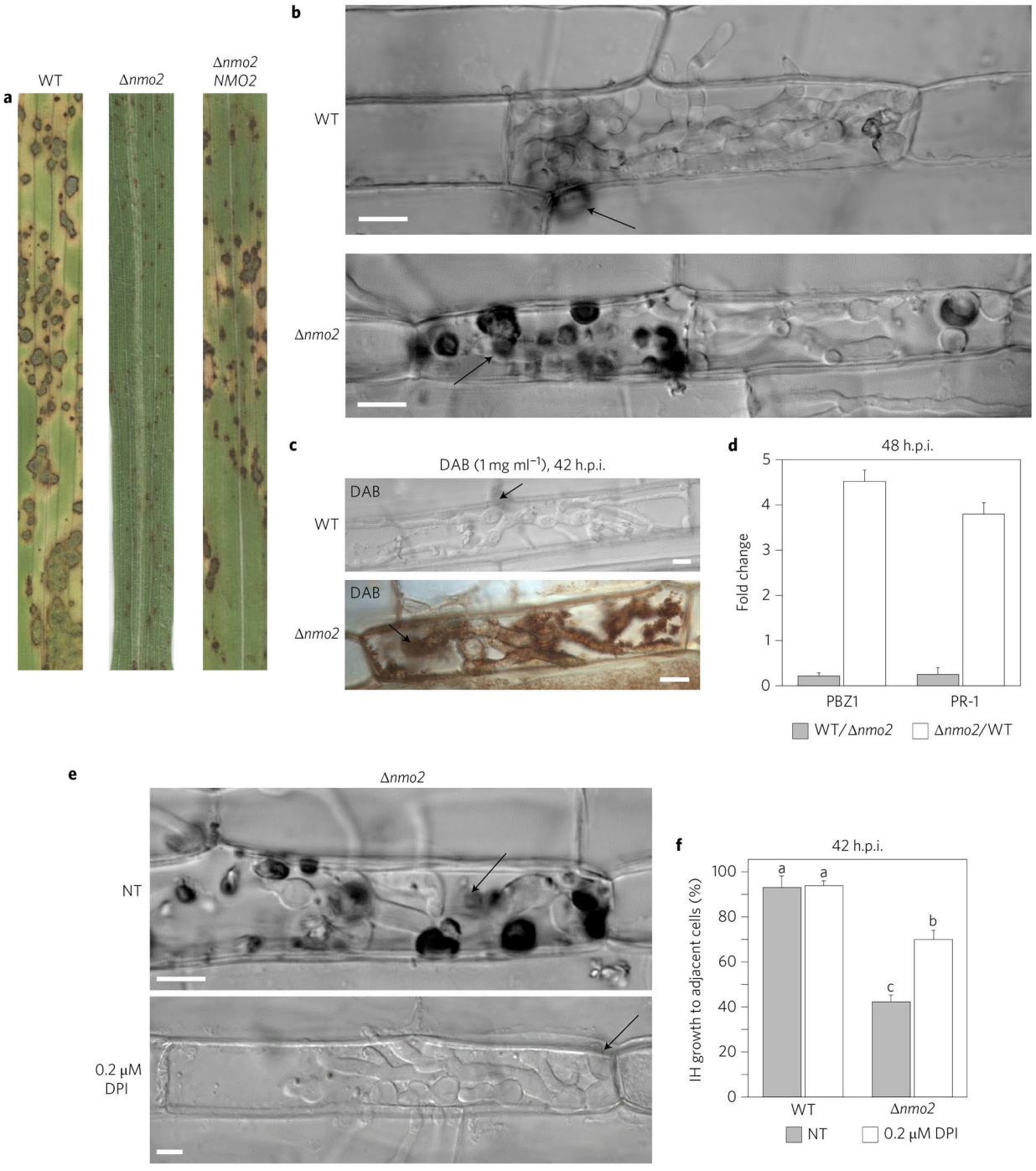
a
WT
Δnmo2
Δnmo2 NMO2
b
WT
Δnmo2
c
DAB (1 mg ml−1), 42 h.p.i.
DAB
WT
DAB
Δnmo2
d
48 h.p.i.
Fold change
0
1
2
3
4
5
PBZ1
PR-1
WT/Δnmo2
Δnmo2/WT
e
Δnmo2
NT
0.2 μM DPI
f
42 h.p.i.
IH growth to adjacent cells (%)
0
20
40
60
80
100
a
a
c
b
WT
Δnmo2
NT
0.2 μM DPI

Figure 4. *NMO2* is essential for neutralizing the host ROS burst and suppressing plant innate immune responses. **a)** Δ*nmo2* mutant strains were non-pathogenic on rice. Spore suspensions of each strain were applied to susceptible CO-39 plants at a rate of 1×10^5 spores per ml. Images of infected leaves were taken 120 h.p.i. **b)** Live-cell imaging of detached rice leaf sheaths by confocal laser scanning microscopy showed that, although able to penetrate rice cuticles, the growth of the Δ*nmo2* mutant in rice cells, compared to WT, was restricted and triggered the formation of cellular deposits inside the first infected cell. **c)** The Δ*nmo2* mutant strain elicited H_2O_2 accumulation in infected rice cells. Infected leaf sheaths were stained with 3,3-diaminobenzidine (DAB) at 42 h.p.i. **d)** Transcript analysis at 48 h.p.i. of the rice pathogenesis related genes *PBZ1* and *PR-1* showed that the Δ*nmo2* mutant elicited stronger plant responses than WT. *PBZ1* and *PR1* expression was analyzed by qPCR on cDNAs acquired from infected leaf sheaths and normalized against the expression of the rice actin-encoding gene *OsACT2*. Fold changes were calculated between strains. Values are the average of three technical replicates performed on cDNAs synthesized from a combined pool of RNA from six biological replicates. Error bars indicate standard deviation. **e & f)** Treatment of spores with 0.2 μM of the NADPH oxidase inhibitor diphenylene iodonium (DPI) prevented the host ROS burst. This suppressed host defense responses and promoted Δ*nmo2* growth in rice cells. NT, no treatment. In **b**, **c** and **e**, live-cell images of infected detached rice leaf sheaths were taken at 42 h.p.i. Black arrows indicate appressoria on the surface of the leaf and the penetration site. Scale bars, 5 μm. **f)** The percentage of IH growing to neighboring cells was calculated by counting how many penetration sites resulted in IH moving to adjacent cells by 42 h.p.i. Values are the mean of three biological replicates, and each replicate consists of 50 penetration sites. Error bars indicate standard deviation. Bars with different letters are significantly different (ANOVA, $P < 0.0001$; least significant difference, 6.2209).

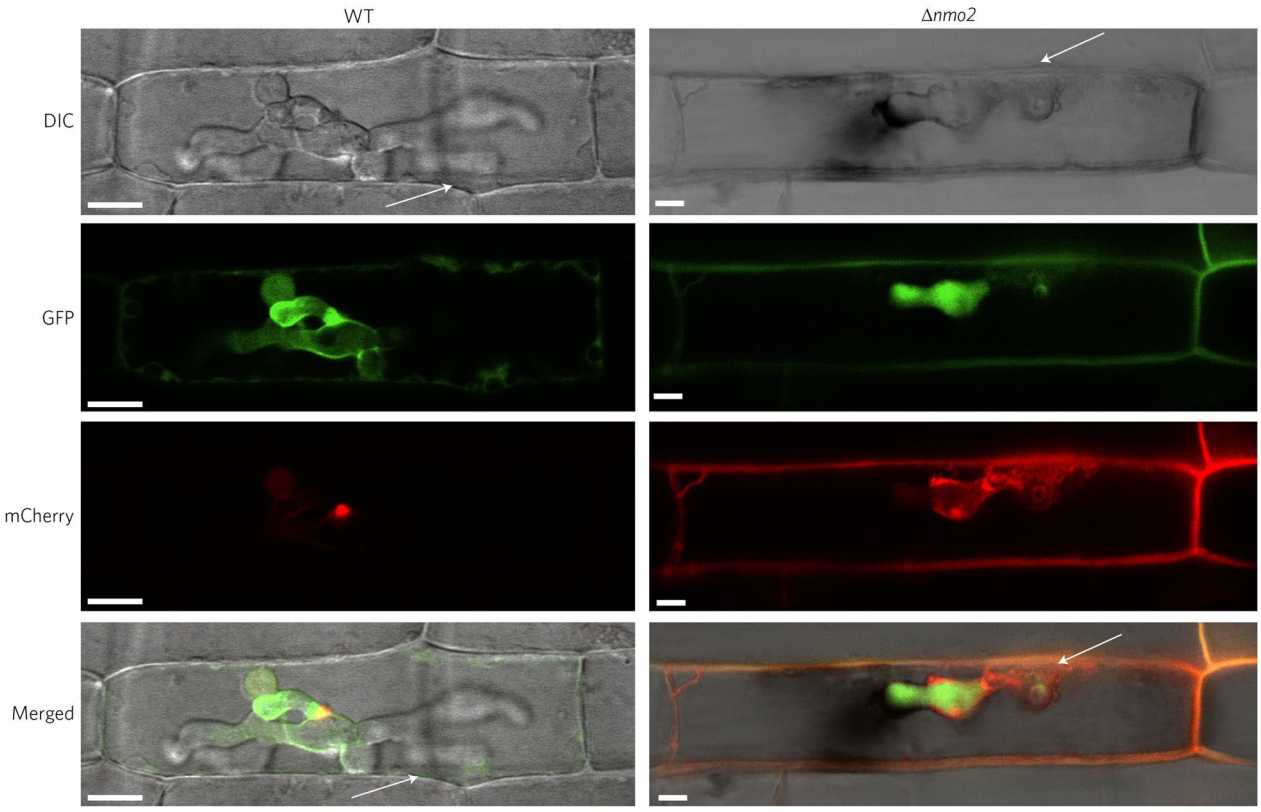

Figure 5. The Pwl2 effector is mislocalized in Δ*nmo2* mutant strains during early rice infection. Detached rice leaf sheaths were inoculated with spores of WT and Δ*nmo2* strains expressing Bas4:GFP and Pwl2:mCherry:NLS. Live-cell imaging by laser scanning confocal fluorescent microscopy was performed at 32 h.p.i. on at least six independent leaf sheaths for each strain. Filter settings: GFP (excitation 488 nm, emission 500–550 nm) and mCherry (excitation 561 nm, emission 575–625 nm). White arrows indicate appressoria on the surface of the leaf and the penetration site. DIC, differential interference contrast. Scale bars, 5 μm.

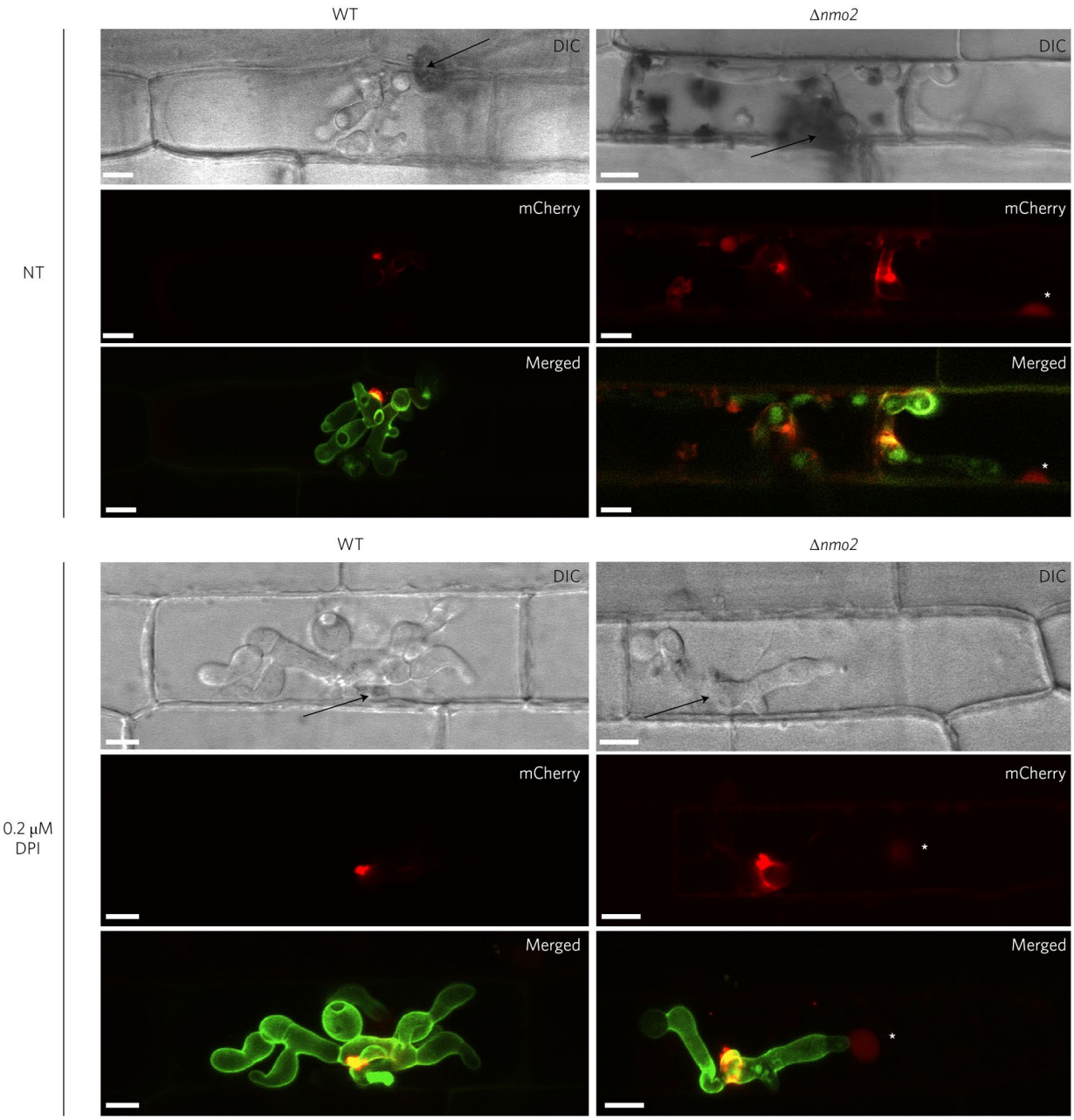

Figure 6. Δ*nmo2* mutant strains develop multiple BIC foci by late rice infection. Detached rice leaf sheaths were inoculated with spores of WT and Δ*nmo2* strains expressing Bas4:GFP and Pwl2:mCherry:NLs. Live-cell imaging by laser scanning confocal fluorescent microscopy was performed at 38 h.p.i. on at least six independent leaf sheaths for each strain. Filter settings: GFP (excitation 488 nm, emission 500–550 nm) and mCherry (excitation 561 nm, emission 575–625 nm). Black arrows indicate appressoria on the surface of the leaf and the penetration site. White asterisks indicate rice nuclei accumulating Pwl2:mCherry:NLS. NT, no treatment. Scale bars, 5 μm.

Acknowledgments — The authors thank B. Valent (Kansas State University) for the gift of pBV591. This work was supported by grants from the National Science Foundation (IOS-1557943) and the USDA-NIFA (2014-67013-21559) to R.A.W. A UNL ARD bridging fund award supported M.M.-G.

Author contributions — R.A.W. conceived the project, designed the experiments and interpreted the data. M.M.-G., D.H., J.D.W., C.E., T.J.B. and R.A.W. performed experiments and analyzed the data. R.A.W. wrote the manuscript. The authors declare no competing financial interests.

References

1. Wilson, R. A. & Talbot, N. J. Under pressure: investigating the biology of plant infection by *Magnaporthe oryzae*. *Nat. Rev. Microbiol.* **7,** 185–195 (2009).
2. Fernandez, J. & Wilson, R. A. Why no feeding frenzy? Mechanisms of nutrient acquisition and utilization during infection by the rice blast fungus *Magnaporthe oryzae*. *Mol. Plant Microbe Interact.* **25,** 1286–1293 (2012).
3. Martin-Urdiroz, M., Oses-Ruiz, M., Ryder, L. S. & Talbot, N. J. Investigating the biology of plant infection by the rice blast fungus *Magnaporthe oryzae*. *Fungal Genet. Biol.* **90,** 61–68 (2016).
4. Ryder, L. S. & Talbot, N. J. Regulation of appressorium development in pathogenic fungi. *Curr. Opin. Plant Biol.* **26,** 8–13 (2015).
5. Marroquin-Guzman, M. & Wilson, R. A. GATA-dependent glutaminolysis drives appressorium formation in *Magnaporthe oryzae* by suppressing TOR inhibition of cAMP/PKA signaling. *PLoS Pathog.* **11,** e1004851 (2015).
6. Dagdas, Y. F. *et al.* Septin-mediated plant cell invasion by the rice blast fungus, *Magnaporthe oryzae*. *Science* **336,** 1590–1595 (2012).
7. Kankanala, P., Czymmek, K. & Valent, B. Roles for rice membrane dynamics and plasmodesmata during biotrophic invasion by the blast fungus. *Plant Cell* **19,** 706–724 (2007).
8. Fernandez, J. & Wilson, R. A. Cells in cells: morphogenetic and metabolic strategies conditioning rice infection by the blast fungus *Magnaporthe oryzae*. *Protoplasma* **251,** 37–47 (2014).
9. Park, C.-H. *et al.* The *Magnaporthe oryzae* effector AvrPiz-t targets the RING E3 ubiquitin ligase APIP6 to suppress pathogen-associated molecular patterntriggered immunity in rice. *Plant Cell* **24,** 4748–4762 (2012).
10. Mentlak, T. A. *et al.* Effector-mediated suppression of chitin-triggered immunity by *Magnaporthe oryzae* is necessary for rice blast disease. *Plant Cell* **24,** 322–335 (2012).
11. Giraldo, M. C. *et al.* Two distinct secretion systems facilitate tissue invasion by the rice blast fungus *Magnaporthe oryzae*. *Nat. Commun.* **4,** 1996 (2013).
12. Fernandez, J., Marroquin-Guzman, M. & Wilson, R. A. Mechanisms of nutrient acquisition and utilization during fungal infections of leaves. *Ann. Rev. Phytopathol.* **52,** 155–174 (2014).
13. Chi, M. H., Park, S. Y., Kim, S. & Lee, Y. H. A novel pathogenicity gene is required in the rice blast fungus to suppress the basal defenses of the host. *PLoS Pathog.* **5,** e1000401 (2009).
14. Huang, K., Czymmek, K. J., Caplan, J. L., Sweigard, J. A. & Donofrio, N. M. *HYR1*-mediated detoxification of reactive oxygen species is required for full virulence in the rice blast fungus. *PLoS Pathog.* **7,** e1001335 (2011).
15. Donofrio, N. M. & Wilson, R. A. Redox and rice blast: new tools for dissecting molecular fungal–plant interactions. *New Phytol.* **201,** 367–369 (2014).

16. Fernandez, J. *et al.* Plant defense suppression is mediated by a fungal sirtuin during rice infection by *Magnaporthe oryzae*. *Mol. Micro.* **94,** 70–88 (2014).
17. Fernandez, J. *et al.* Principles of carbon catabolite repression in the rice blast fungus: Tps1, Nmr1-3, and a MATE-family pump regulate glucose metabolism during infection. *PLoS Genet.* **8,** e1002673 (2012).
18. Fernandez, J. & Wilson, R. A. Characterizing roles for the glutathione reductase, thioredoxin reductase and thioredoxin peroxidase-encoding genes of *Magnaporthe oryzae* during rice blast disease. *PLoS ONE* **9,** e87300 (2014).
19. Dean, R. A. *et al.* The genome sequence of the rice blast fungus *Magnaporthe grisea*. *Nature* **434,** 980–986 (2005).
20. Wilson, R. A. & Arst, H. N. Jr. Mutational analysis of AREA, a transcriptional activator mediating nitrogen metabolite repression in *Aspergillus nidulans* and a member of the 'streetwise' GATA family of transcription factors. *Microbiol. Mol. Biol. Rev.* **62,** 586–596 (1998).
21. Wilson, R. A., Gibson, R. P., Quispe, C. F., Littlechild, J. A. & Talbot, N. J. An NADPH-dependent genetic switch regulates plant infection by the rice blast fungus. *Proc. Natl Acad. Sci. USA* **107,** 21902–21907 (2010).
22. Wilson, R. A. *et al.* Tps1 regulates the pentose phosphate pathway, nitrogen metabolism and fungal virulence. *EMBO J.* **26,** 3673–3685 (2007).
23. Marcos, A. T. *et al.* Nitric oxide synthesis by nitrate reductase is regulated during development in *Aspergillus*. *Mol. Microbiol.* **99,** 15–33 (2016).
24. Corpas, F. J. & Barroso, J. B. Nitro-oxidative stress vs oxidative or nitrosative stress in higher plants. *New Phytol.* **199,** 633–635 (2013).
25. O'Donnell, V. B. & Freeman, B. A. Interactions between nitric oxide and lipid oxidation pathways: implications for vascular disease. *Circ. Res.* **88,** 12–21 (2001).
26. Pacher, P., Beckman, J. S. & Liaudet, L. Nitric oxide and peroxynitrite in health and disease. *Physiol. Rev.* **87,** 315–424 (2007).
27. Vandelle, E. & Delledonne, M. Peroxynitrite formation and function in plants. *Plant Sci.* **181,** 534–539 (2011).
28. Nathan, C. The moving frontier in nitric oxide-dependent signaling. *Sci. STKE* **2004,** pe52 (2004).
29. Rubbo, H. & Radi, R. Protein and lipid nitration: role in redox signaling and injury. *Biochim. Biophys. Acta* **1780,** 1318–1324 (2008).
30. Batinić-Haberle, I. *et al.* Pure MnTBAP selectively scavenges peroxynitrite over superoxide: comparison of pure and commercial MnTBAP samples to MnTE-2-PyP in two different models of oxidative stress injuries, SOD-specific *E. coli* model and carrageenan-induced pleurisy. *Free Radic. Biol. Med.* **46,** 192–201 (2009).
31. Radi, R., Beckman, J. S., Bush, K. M. & Freeman, B. A. Peroxynitrite-induced membrane lipid peroxidation: the cytotoxic potential of superoxide and nitric oxide. *Arch. Biochem. Biophys.* **288,** 481–487 (1991).
32. Ischiropoulos, H. Biological tyrosine nitration: a pathophysiological function of nitric oxide and reactive oxygen species. *Arch. Biochem. Biophys.* **356,** 1–11 (1998).
33. Hao, P. *et al.* Herbivore-induced callose depositions on the sieve plates of rice: an important mechanism for host resistance. *Plant Physiol.* **146,** 1810–1820 (2008).
34. Khang, C. H. *et al.* Translocation of *Magnaporthe oryzae* effectors into rice cells and their subsequent cell-to-cell movement. *Plant Cell* **22,** 1388–13403 (2010).
35. Brown, A. J., Haynes, K. & Quinn, J. Nitrosative and oxidative stress responses in fungal pathogenicity. *Curr. Opin. Microbiol.* **12,** 384–391 (2009).
36. Francis, K., Russell, B. & Gadda, G. Involvement of a flavosemiquinone in the enzymatic oxidation of nitroalkanes catalyzed by 2-nitropropane dioxygenase. *J. Biol. Chem.* **280,** 5195–51204 (2005).

37. Bellin, D., Asai, S., Delledonne, M. & Yoshioka, H. Nitric oxide as a mediator for defense responses. *Mol. Plant Microbe Interact.* **26,** 271–277 (2013).
38. Li, G., Marroquin-Guzman, M. & Wilson, R. A. Chromatin immunoprecipitation (ChIP) assay for detecting direct and indirect protein–DNA interactions in *Magnaporthe oryzae*. *Bio Protoc* **5,** e1643 (2015).
39. Kido, T., Soda, K., Suzuki, T. & Asada, K. A new oxygenase, 2-nitropropane dioxygenase of *Hansenula mrakii*. Enzymologic and spectrophotometric properties. *J. Biol. Chem.* **251,** 6994–7000 (1976).
40. Grossi, L. & D'Angelo, S. Sodium nitroprusside: mechanism of NO release mediated by sulfhydryl-containing molecules. *J. Med. Chem.* **48,** 2622–2626 (2005).

Supplementary information follows.

The *Magnaporthe oryzae* nitrooxidative stress response suppresses rice innate immunity during blast disease

Margarita Marroquin-Guzman[1], David Hartline[1], Janet D. Wright[1], Christian Elowsky[2], Travis J. Bourret[3], Richard A. Wilson[1*]

[1]Department of Plant Pathology, University of Nebraska-Lincoln, Lincoln, Nebraska

[2]Department of Agronomy and Horticulture, University of Nebraska–Lincoln, Lincoln, Nebraska

[3]Department of Medical Microbiology and Immunology, Creighton University, Omaha, Nebraska

*rwilson10@unl.edu

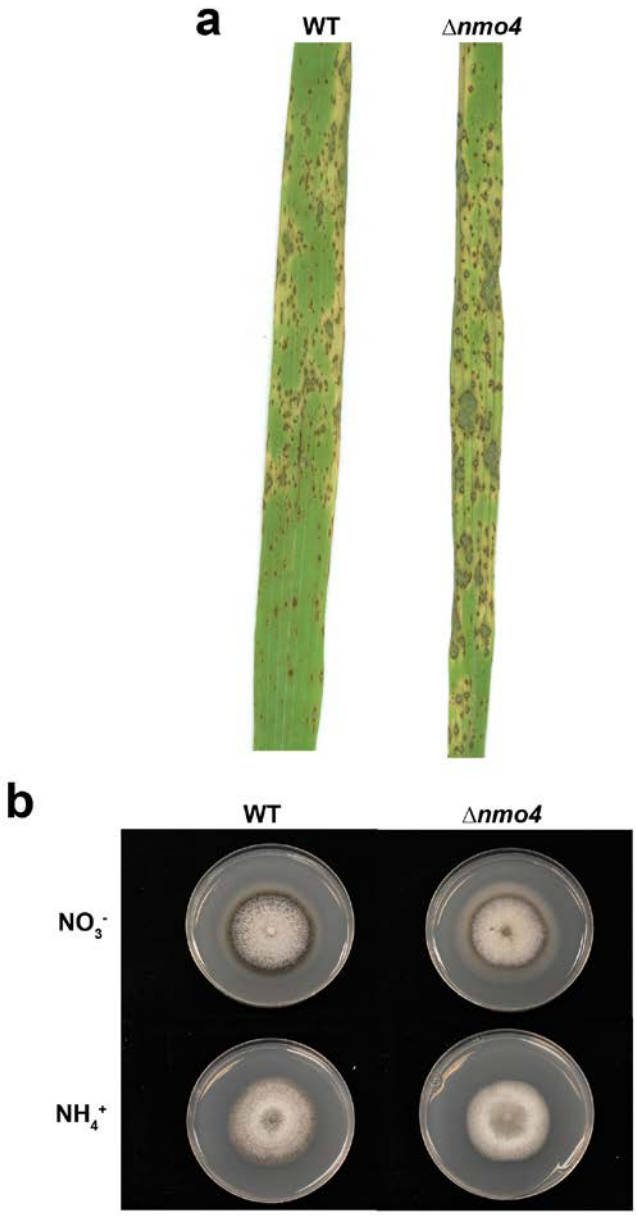

Supplementary Figure 1. *NMO4* is not required for pathogenicity and growth on nitrate. a, Spore suspensions of each strain were applied to three weeks old rice seedlings (CO-39). **b**, Radial growth of *Δnmo4* mutant strains was tested compared to wild type (WT) on 85 mm plates with minimal media containing 1% (w/v) glucose and 10 mM of the indicated nitrogen source. Representative images from three replicates were taken 10 days after inoculation.

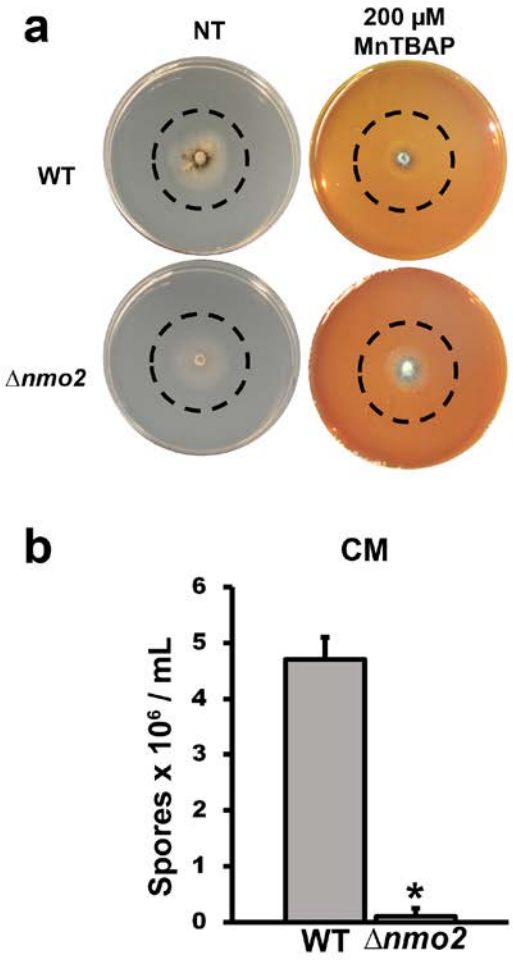

Supplementary Figure 2. **Loss of *NMO2* affects growth and sporulation. a**, Growth of the *Δnmo2* mutant on GMM with NO_3^- as a sole nitrogen source was restored relative to WT when MnTBAP was added to the media. Selected areas (diameter: 35 mm) in the 85 mm plates indicate the cropped images shown in Fig. 3e. NT= no treatment. Representative images from three replicates were selected. **b**, Sporulation rates of the *Δnmo2* mutant strain was significantly reduced compared to WT after growth on complete media (two tailed *t-test*, *, $P < 0.0001$). Fungal spores were isolated from 12 days old plate cultures, repeated in triplicate for each strain. Error bars are standard deviation.

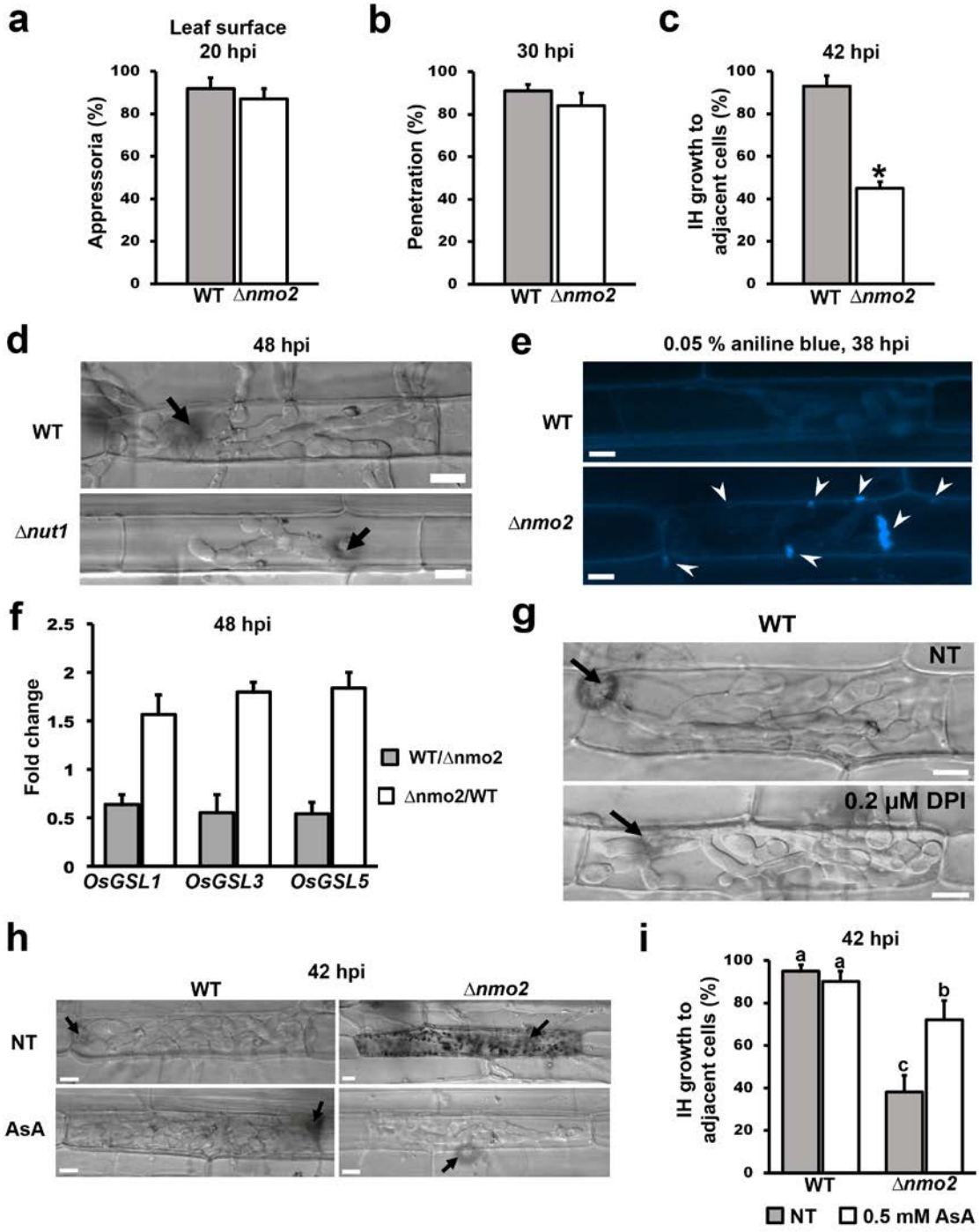

Supplementary Figure 3. *NMO2* is essential for neutralizing the host ROS burst, suppressing plant defenses and colonizing rice cells. On detached rice leaf sheaths, spores of the Δ*nmo2* mutant strain had formed appressoria by 20 hpi (**a**), and had penetrated into rice epidermal cells by 30 hpi (**b**), with the same rates as WT (two tailed *t-test*, *P*: 0.1577 and two tailed *t-test*, *P*: 0.733, respectively). However, (**c**) the Δ*nmo2* mutant was impaired in its ability to grow IH into cells adjacent to the point of entry. **d,** At 48

hpi, the Δ*nut1* mutant strain was impaired for growth in rice cells compared to WT, and did not elicit the formation of cellular deposits. **e.**, Staining with aniline blue revealed the formation of callose deposits (arrowheads) in the rice cell wall in response to Δ*nmo2* infection. Scale bar is 5 μm. **f,** Rice callose synthase-encoding genes were upregulated in the Δ*nmo2* infected rice leaf sheaths compared to WT. Expression was normalized against the *MoACT1* gene, and the values are the average of three technical replicates with standard deviation. **g**, WT infection of rice cells was not affected by treatment with 0.2 μM of the NADPH oxidase inhibitor diphenylene iodonium (DPI). **h**, **i**, Treatment with 0.5 mM L- ascorbic acid sodium salt (AsA) quenched the host ROS burst. This suppressed plant defense responses (**h**) and promoted the *in planta* growth of the Δ*nmo2* mutant relative to the untreated control (**i**). **d**,**g,h**, Live-cell images were taken at 48 hpi (**d**) and 42 hpi (**g,h**), black arrows indicate appressoria on the surface of the leaf and the penetration site. NT= no treatment. Scale bar is 5 μm. **a**,**b**, Appressorium formation rates were calculated from 50 spores per leaf sheath, repeated in triplicate, at 24 hpi. Appressorium penetration rates were calculated from 50 appressoria per leaf sheath, repeated in triplicate, at 24 hpi. **c**, **i**, The percentage of infectious hypha (IH) growth to neighboring cells was calculated by counting how many penetration sites resulted in IH moving to adjacent cells by 42 hpi. Values are the mean of three biological replicates; each replicate consisted of 50 penetration sites. **i,** Bars with different letters are significantly different (ANOVA, $P < 0.0001$, LSD: 5.7262). **a-c**, **f**, **i,** Error bars denote standard deviation.

Supplementary Table 1. *Magnaporthe oryzae* strains used in this study.

Strains	Genotype	Reference
Guy11	*M. oryzae* wild type isolate (WT) used throughout this study.	Wilson et al. 2010
Δ*nmo2*	Nitronate monooxygenase 2 (MGG_02439) deletion mutant of Guy11. Sulphonylurea resistant.	*This study*
Δ*nmo2 NMO2*	Complementation strain resulting from integration of the full length *NMO2* gene in to the Δ*nmo2* genome. Sulphonylurea resistant.	*This study*
Δ*nmo4*	Nitronate monooxygenase 4 (MGG_09511) deletion mutant of Guy11. Sulphonylurea resistant.	*This study*
Δ*tps1*	Trehalose-6-phosphate synthase 1 deletion mutant of Guy11. Sulphonylurea resistant.	Fernandez et al. 2012
Δ*nut1*	Nitrogen metabolite repression mutant of Guy11. Sulphonylurea resistant.	Fernandez et al. 2012
WT Bas4:GFP Pwl2:mCherry:NLS	WT strain expressing pBV591 (Giraldo et al. 2013).	*This study*
Δ*nmo2* Bas4:GFP Pwl2:mCherry:NLS	Δ*nmo2* mutant strain expressing pBV591 (Giraldo et al. 2013).	*This study*

Fernandez, J. *et al.* Principles of carbon catabolite repression in the rice blast fungus: Tps1, Nmr1-3, and a MATE–Family Pump regulate glucose metabolism during Infection. *PLoS Genet.* **8**, e1002673 (2012). doi: 10.1371/journal.pgen.1002673.

Giraldo, M.C. *et al.* Two distinct secretion systems facilitate tissue invasion by the rice blast fungus Magnaporthe oryzae. *Nat. Commun.* **4**,1996 (2013).

Wilson, R.A., Gibson, R.P., Quispe, C.F., Littlechild, J.A. & Talbot, N.J. An NADPH-dependent genetic switch regulates plant infection by the rice blast fungus. *Proc. Natl. Acad. Sci. U. S. A.* **107**, 21902–21907 (2010).

Supplementary Table 2. Oligonucleotide primers used in this study.

Gene	Primer	Sequence 5' – 3'
ILV1[1]	M13F:IL[2]	**CGCCAGGGGTTTTCCCAGTCACGAC**GTCGACGTGCCAACGCCACAG
	ILSplit	AAGCATGTGCAGTGCCTTC
	M13R:LV1[2]	**AGCGGATAACAATTTCACACAGGA**GTCGACGTGAGAGCATGCTAA
	LV1Split	CGCCCGGCCGACATCC
NMO2	NMO2-LF5' [3]	CGCAGGAGGGAGGCAGCA
	NMO2-LF3' [2,3]	**GTCGTGACTGGGAAAACCCTGGCG**TGTGGGATTTTATTTTGTCTTTTGTTGG
	NMO2-RF5'[2,3]	**TCCTGTGTGAATTGTTATCCGCT**GTGAGGTCAATGGTTGCCGAGG
	NMO2-RF3' [3]	ACCACTGACAAGAGTCGCCAAACA
	NMO2-nesF [3]	AAGTAAGTGAAGCGGGCTCGGA
	NMO2-nesR [3]	TCATCCCCCGCAACCAACC
NMO4	NMO4-LF5' [3]	AAGCGAGACAGCCGAGATGGAG
	NMO4-LF3' [2,3]	**GTCGTGACTGGGAAAACCCTGGCG**CTTTGCTCTATGGTTGGACTGTGAACT
	NMO4-RF5'[2,3]	**TCCTGTGTGAAATTGTTATCCGCT**CTCTGGTGAGCGGTCAGCGTG
	NMO4-RF3' [3]	TCAACCGTCAGTGCTCGTCTGG
	NMO4-nesF [3]	TCGGTCCAGGTCCAGGTTCAAG
	NMO4-nesR [3]	GATGAGCACAAACTACGGGTAAGTCTTC
NMO2	Nmo2 F[4]	GCTGTGTGACAAGGGCATCGTG
	Nmo2 R[4]	ACCTGCTCTTCTGCGTATCACCC
NMO1	Nmo1 F[4]	TGCTGCTGCTCTGGCTCTTGG
	Nmo1 R[4]	TGACTCCTTGGCTTGATTGAACCTC
NMO3	Nmo3 F[4]	CGCCAACTCGCCCCACC
	Nmo3 R[4]	GTGTCGGTGGCGTCGTGGT
NMO4	Nmo4 F[4]	AACACCACTCGTCTTTACCGCAAC
	Nmo4 R[4]	TAGTCTGGGTCGCCGTTGATAAATAC
NMO5	Nmo5 F[4]	GGGTTGGCACACGCTTCATCC
	Nmo5 R[4]	CTTCTTGTCATCCTTGCCCTTGG
NIA1	Nia1 F[4]	TGGCAACCGAACAGAGGAAGAC
	Nia1 R[4]	TCAGAAAAACAACAAATCATCATCCTTCC
NII1	Nii1 F[4]	CTCTCCATCGCCACCTTTGAGG
	Ni11 R[4]	TCACCAATCCGGCGCG
PBZ1	Pbz1 F[4]	CTACTATGGCATGCTCAAGAT+D1982
	Pbz1R[4]	ATAGAAAGGCACATAAACACAA
PR-1	Pr-1 F[4]	TCTTCATCACCTGCAACTACTC
	Pr-1 R[4]	ATTCATCGGATTTATTCTCACC
OsACT2	Rice ACT-U1[4]	CTTCAACACCCCTGCTATG
	Rice ACT- L1[4]	CCGTTGTGGTGAATGAGTAA
OsGSL1	OsGSL1-F[4, 5]	TGAGGACCTGCCACGATT
	OsGSL1-R[4, 5]	CACGCTGATTGCGAACAT
OsGSL3	OsGSL3-F[4, 5]	TGGCAAGCGACCACATAG
	OsGSL3-R[4, 5]	AGACCTTAGCACGGACTG
OsGSL5	OsGSL5-F[4, 5]	GTGGTGTCCCTGCTATGA
	OsGSL5-R[4, 5]	GTTGTTTGCTATTCTCCC
MoACT1	MgActin F[4]	ACTCCTGCTTCGAGATCCACATC
	MgActin R[4]	TCGACGTCCGAAAGGATCTGT
TUB2	QRT-PCR b-tub F2[4]	CGCGGCCTCAAGATGTCGT

	QRT-PCR b-tub R2 [4]	GCCTCCTCCTCGTACTCCTCTTCC
hph	Hyg-int 5 Fw[6]	CGTCGATAAATGGGCGTCCTGTAT
	Hyg-int 3 Rev[6]	CAGAAGAAGATGT

[1] Sulphonylurea resistance gene amplification. [2]M13F/M13R sequences, highlighted in bold, are upstream of the gene specific sequences, respectively (Wilson et al, 2010). [3]Primers for split marker deletion construct (Wilson et al, 2010). [4]Primers used for qRT-PCR analysis. [5] Primers used to quantify the expression of rice callose synthase-encoding genes (Hao et al, 2008). [6] Primers used for screening of hygromycin resistance strains carrying the plasmid pBV591, expressing Pwl2:mCherry:NLS and Bas4: GFP (Giraldo et al, 2013).

Hao, P. *et al*. Herbivore-induced callose depositions on the sieve plates of rice: an important mechanism for host resistance. *Plant Physiol*. **146,** 1810-1820 (2008).

Giraldo, M.C. *et al.* Two distinct secretion systems facilitate tissue invasion by the rice blast fungus *Magnaporthe oryzae*. *Nat. Commun.* **4**,1996 (2013).

Wilson, R.A., Gibson, R.P., Quispe, C.F., Littlechild, J.A. & Talbot, N.J. An NADPH-dependent genetic switch regulates plant infection by the rice blast fungus. *Proc. Natl. Acad. Sci. U. S. A.* **107**, 21902–21907 (2010).